The Toronto traumatic brain injury study

Injury severity and quantified MRI

B. Levine, PhD
N. Kovacevic, PhD
E.I. Nica, BSc
G. Cheung, MD
F. Gao, MD
M.L. Schwartz, MD
S.E. Black, MD

Address correspondence and reprint requests to Dr. Brian Levine, The Rotman Research Institute at Baycrest, 3560 Bathurst St., Toronto, ON M6A 2E1, Canada
blevine@rotman-baycrest.on.ca

ABSTRACT

Objective: To assess the relationship between regional brain volume changes and traumatic brain injury (TBI) severity in patients with and without focal lesions.

Methods: Sixty-nine chronic-phase TBI patients spanning the full range of severity were recruited from consecutive hospital admissions. Patients received high-resolution structural MRI a minimum of 1 year after injury. Multivariate statistical analyses assessed covariance patterns between volumes of gray matter, white matter, and sulcal/subdural and ventricular CSF across 38 brain regions and TBI severity as assessed by depth of coma at the time of injury. Patients with diffuse and diffuse plus focal injury were analyzed both separately and together.

Results: There was a stepwise, dose–response relationship between parenchymal volume loss and TBI severity. Patients with moderate and severe TBI were differentiated from those with mild TBI, who were in turn differentiated from noninjured control subjects. A spatially extensive pattern of volume loss covaried with TBI severity, with particularly widespread effects in white matter volume and sulcal/subdural CSF. The most reliable effects were observed in the frontal, temporal, and cingulate regions, although effects were observed to varying degrees in nearly every brain region. Focal lesions were associated with greater volume loss in frontal and temporal regions, but volume loss remained marked even when analyses were restricted to patients with diffuse injury.

Conclusions: Patterns of parenchymal volumetric changes can differentiate among levels of traumatic brain injury (TBI) severity, even in mild TBI. TBI causes a spatially extensive pattern of volume loss that reflects independent but overlapping contributions of focal and diffuse injury.
***Neurology*® 2008;70:771–778**

GLOSSARY

DAI = diffuse axonal injury; **FCC** = focal cortical contusion; **FOV** = field of view; **GCS** = Glasgow Coma Scale; **IQR** = intraquartile range; **LOC** = loss of consciousness; **LV** = latent variable; **NEX** = number of excitations; **PLS** = partial least squares; **PTA** = post-traumatic amnesia; **sCSF** = sulcal/subdural CSF; **TBI** = traumatic brain injury; **TE** = echo time; **TR** = repetition time; **TSI** = time since injury; **vCSF** = ventricular CSF.

Traumatic brain injury (TBI) is one of the commonest neurologic disorders[1] and a leading cause of disability.[2] This disability is largely attributable to the cognitive and behavioral consequences of TBI neuropathology that affects independence, productivity, and quality of life.[3] Accurate characterization of neuropathology is critical to assessment and rehabilitation in TBI.

TBI neuropathology can be characterized as either focal or diffuse.[4] Focal injury often results from inertial forces causing localized contusional damage in ventral and polar frontal and anterior temporal areas.[5,6] Diffuse axonal injury (DAI) is caused by ionic homeostatic disruption and changed permeability of the axolemma, terminated hours later by axonal disconnection and demise of the distal axonal segment.[7]

Supplemental data at www.neurology.org

From the Rotman Research Institute (B.L., N.K., E.I.N., S.E.B.) Baycrest Centre for Geriatric Care, Toronto; Departments of Psychology (B.L.), Medicine (Neurology) (B.L., S.E.B.), and Surgery (Neurosurgery) (M.L.S.), University of Toronto; and Departments of Diagnostic Imaging and Radiology (G.C.), Medicine (Neurology) (F.G., S.E.B.), L.C. Campbell Cognitive Neurology Research Unit and Heart and Stroke Foundation Center for Stroke Recovery (F.G., S.E.B.), Surgery (Neurosurgery) (M.L.S.), and Imaging Research (S.E.B.), Sunnybrook Health Sciences Centre, Toronto, Ontario, Canada.

Supported by grants from the Canadian Institutes of Health Research (grants MT-14744, MOP-37535, and MOP-108540 to B.L. and grant MT13129 to S.E.B.) and the NIH–National Institute of Child Health and Human Development (grant HD42385-01) to B.L.

Disclosure: The authors report no conflicts of interest.

Table Characteristics of patients with TBI and controls

		Age, y		Education, y		GCS score		Duration of LOC, h		Duration of PTA, d		TSI, y	
Group	n*	Mean	SD	Mean	SD	Mean	SD	Median	IQR	Median	IQR	Mean	SD
Mild	13 (8)	33.7	13.1	13.2	2.0	14.6	0.7	0.00	0–0.13	0.0	0–0.30	1.19	0.42
Moderate	30 (16)	32.0	11.1	14.9	2.3	11.1	2.0	25.0	2.25–126	8.5	3–21	1.22	0.66
Severe	26 (19)	28.9	8.0	14.4	2.7	6.7	2.6	96	54–336	28	19–60	1.64	1.3
Controls	12 (7)	27.2	3.3	20.1	2.5	NA	NA	NA	NA	NA	NA	NA	NA

* Number of males in parentheses.
TBI = traumatic brain injury; GCS = Glasgow Coma Scale; LOC = loss of consciousness; PTA = post-traumatic amnesia; TSI = time since injury; IQR = intraquartile range; NA = not applicable.

Detection of lasting TBI neuropathology is best in the chronic phase, after stabilization of acute and subacute pathology.[8] Large focal cortical contusions (FCCs) are readily appreciated on structural anatomic images, whereas detection of DAI is less straightforward. Hemorrhagic "DAI" lesions detected on structural T2-weighted or gradient echo MRI scans represent only the regions where the confluence of damage is sufficient to be detected by the naked eye.[9] In many cases, DAI can only be detected microscopically.[10,11] Although DAI is not directly assessed in vivo, its effects can be detected indirectly on structural images by measuring volume loss in selected structures.[12-15] Tissue compartment segmentation algorithms that separate tissue types based on MRI signal intensity have been used to quantify volume loss across the different brain tissue compartments.[16,17] These algorithms can be combined with region-of-interest or voxel-based measures to assess localized volume loss due to DAI.[18-21]

While advances in MRI technology and image analysis have improved in vivo assessment of TBI neuropathology, there have been few systematic studies of large samples of patients across the range of TBI severity. In this study, we comprehensively assessed chronic-phase TBI neuropathology as measured by MRI in a sample of patients that is large relative to previous reports. We combined a robust tissue compartment segmentation procedure with regional brain parcellation to quantify localized volume changes, including separate assessment of sulcal/subdural and ventricular CSF compartments. Finally, we dissociated the effects of diffuse injury from combined focal and diffuse injury.

METHODS

Participants. Sixty-nine TBI patients were recruited from consecutive admissions to Sunnybrook Health Sciences Centre, Canada's largest trauma center, at approximately 1 year after injury. Eighty percent (55) of the patients sustained their TBI in a motor vehicle accident. Injury severity was determined by the Glasgow Coma Scale (GCS) as documented at the time of discharge from the trauma unit, corresponding to the recommended 6-hour GCS score.[22] Severity classification (mild/moderate/severe) was upgraded in eight cases where extended loss of consciousness (>2 hours), post-traumatic amnesia (>48 hours), or focal lesions suggested a more severe injury than indicated by the GCS. Twelve healthy age- and sex-matched participants were scanned as a noninjured group. Exclusion criteria for all subjects included significant psychiatric history, substance abuse, learning disability, multiple traumatic brain injuries, severe injury to organs other than the brain, history of neurologic disease, major medical problems or medications impacting cognition, and lack of English proficiency.

As seen in the table, there were no significant differences across groups for age, sex, vocabulary knowledge, and time since injury. There was a significant group difference for education, $F(3,73) = 14.975$, $p < 0.001$, with post hoc tests indicating that the comparison group had significantly higher education than the three TBI groups. All participants were informed of the experimental aim of the study and gave their consent to participate. The study was approved by the local institutional ethics review boards.

MRI acquisition. Participants were scanned with a 1.5-T magnetic resonance (MR) system (Signa, CV/i hardware, LX software, General Electric Healthcare, Waukesha, WI). A sagittal T1-weighted three-dimensional volume technique produced 124 1.3-mm slices (repetition time [TR]/echo time [TE] of 35/5 msec, flip angle of 35 degrees, 1.0 number of excitations [NEX], and field of view [FOV] of 22 cm). Proton density and T2-weighted images with a slice thickness of 3 mm were obtained using an interleaved sequence (TR/TE of 3,000/30, 80 msec, 0.5 NEX, and FOV of 22 cm). For TBI patients, gradient echo T2 sequences with a slice thickness of 6 mm were obtained to emphasize hemosiderin deposits (TR/TE of 750/35 msec, flip angle of 20 degrees, 2.0 NEX,

and FOV of 22 cm). For technical reasons, gradient echo images were unavailable for 21 patients.

Image processing. Brain MRI data were analyzed via an updated version of our previously reported image processing pipeline.[23,24] The main modification to this protocol involved template matching, allowing for comparison of individual images to a standard image and facilitating automation of previously semiautomated steps. The first step in the pipeline was to create an unbiased nonlinear average of T1-weighted images of the 12 matched noninjured participants using a modification of an algorithm previously developed for mouse brain MRI.[25] Each participant's T1-weighted image was then registered to the template brain,[26,27] preserving the original size of the brain while standardizing the position and orientation. Images were resampled into template space using windowed sinc interpolation. Template matching was accomplished via nonlinear registration of T1-weighted images to the template image.[28]

Removal of nonbrain tissue from the image incorporated thresholding information derived from the proton density (PD)–weighted and T2-weighted images, facilitating the distinction between dura mater and gray matter.[23] This is contrasted to methods of brain extraction based on the T1-weighted image that emphasize the cortical surface, inconsistently preserving subdural CSF.

Lesions due to FCC were manually defined slice-by-slice in the axial plane (with occasional corroboration from the coronal plane) using Analyze® software (Biomedical Imaging Resource, Mayo Foundation, Rochester, MN). Traceable lesions appeared on at least two slices, with a minimal diameter of at least 3 mm. When necessary, T2- and PD-weighted images were used to guide the tracing, but only lesions visible on T1-weighted images were traced. We identified traceable lesions in 23 of the 69 patients (11 moderate, 12 severe). These lesions followed a ventral frontal/anterior temporal distribution typical for TBI,[4,5] with a tendency for lateralization to the right hemisphere (figure 1). Scans were clinically interpreted by a board-certified neuroradiologist specializing in TBI. In addition to the large focal lesions, evidence of DAI (e.g., hemosiderin deposits) was present for 91% (51) of the moderate and severe TBI patients and 15% (2) of the mild TBI patients. These estimates were not affected by the unavailability of gradient echo images in 21 patients, because all of these patients had DAI lesions on T2-weighted images.

The voxels on the T1-image were then classified as representing gray matter, white matter, or CSF using a robust automated tissue classification method that corrects for radiofrequency inhomogeneity inherent to MR scanning.[23] A trained operator reclassified CSF-segmented voxels inside the ventricles, allowing for the separate assessment of ventricular and sulcal/subdural CSF (vCSF and sCSF).

A modified semiautomated brain region extraction (SABRE)[24] method was then used to create regions of interest on the template brain. Based on identification of the edges of the brain and the anterior and posterior commissures, a Talairach-like[29] grid is automatically created. The algorithm uses this grid along with the 15 manually identified landmark coordinates and tracing of the cingulate gyrus to divide the brain into 38 regions (19 per hemisphere; figure 2). Nonlinear deformation field matching of the template to individual images was used to customize these regions to fit each participant's brain anatomy (as opposed to transforming images to fit the template, which can distort interindividual topographical variability). Regional gray matter, white matter, and CSF volumes were adjusted for total intracranial capacity using a regression-based method.[30]

Figure 1 Distribution of focal lesions (contusions) in 23 patients with traumatic brain injury

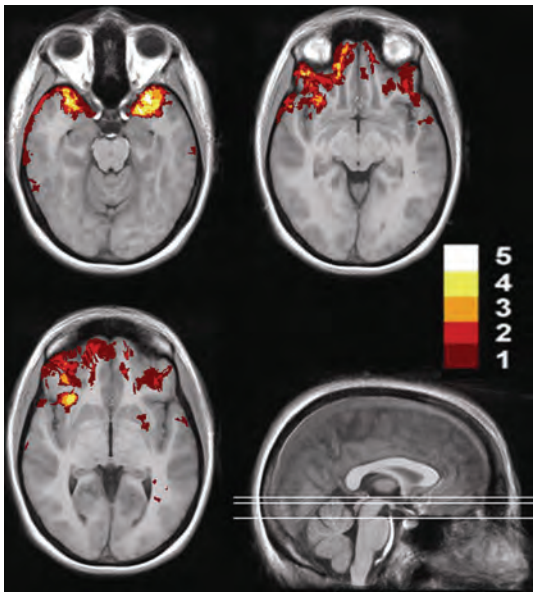

Lesion tracings are projected on selected axial slices of a template brain derived from 12 healthy control subjects. The color scale indicates degree of lesion overlap across patients (max = 5). Lower right sagittal image indicates slice location of the three axial images, with the most ventral axial image appearing in the upper left, the middle axial image in the upper right, and the most dorsal axial image in the lower left.

Our tissue compartment segmentation and SABRE software are particularly well-suited to analysis of brains with atrophy, because they do not require spatial transformation that can distort interindividual topographical variability. These algorithms have been successfully applied to normal aging,[24] multiple sclerosis,[31] and dementia[32] populations.

Image analysis. Partial least squares (PLS) is a flexible multivariate technique that has been extensively applied to brain imaging data.[33,34] Although most of these applications have involved PET and fMRI, it has also been applied to EEG[35,36] and to structural brain imaging data.[32] In general terms, PLS relates two sets of variables to each other. In the present application, it was used to identify patterns of regional volume loss related to TBI severity group. Because PLS considers the brain as a whole, it is well-suited to the detection of distributed patterns of volume loss that covary with injury severity.

In the first step of the PLS analyses, correlations are computed between the brain imaging data (i.e., regional gray matter, white matter, and CSF volumes) and TBI severity group membership (coded as 0 or 1 for each group). Singular value decomposition is then applied to this correlation matrix to identify latent variables (LVs) that indicate optimal relations between TBI severity and patterns of regional brain volume loss.[33,34] Saliences (similar to factor loadings in factor analyses) reflect the contribution of individual brain vol-

Figure 2 SABRE regional cortical divisions in axial and sagittal views

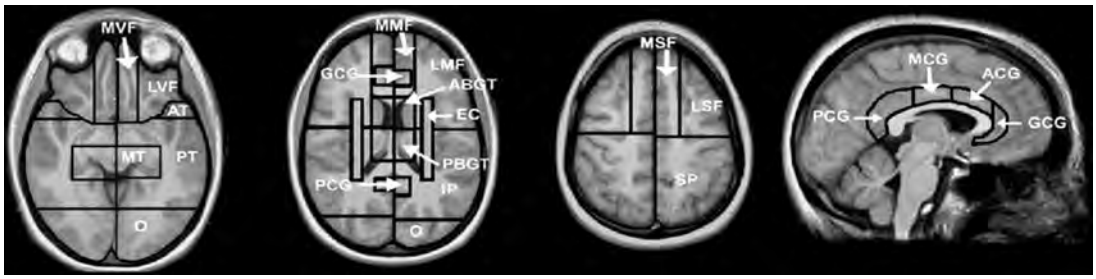

SABRE = semiautomated brain region extraction; LSF = lateral superior frontal; MSF = medial superior frontal; LMF = lateral middle frontal; MMF = medial middle frontal; LVF = lateral ventral frontal; MVF = medial ventral frontal; GCG = genual cingulate gyrus; ACG = anterior cingulate gyrus; MCG = middle cingulate gyrus; PCG = posterior cingulate gyrus/retrosplenial cortex; AT = anterior temporal; MT = medial temporal; PT = posterior temporal; O = occipital; ABGT = anterior basal ganglia/thalamus; PBGT = posterior basal ganglia/thalamus; EC = external capsule/corona radiata; IP = inferior parietal; SP = superior parietal.

umes and group membership to the LV (for details, see references 33 and 34).

The significance of each latent variable was assessed by 1,500 permutation tests[37] in which the observations are randomly reordered without replacement to calculate the probability of each LV having occurred by chance. The stability of each brain region's contribution to the latent variable was determined through bootstrap resampling (subjects were resampled 500 times).[38] Brain regions were considered reliable if they had a ratio of salience to standard error (hereafter referred to as the bootstrap ratio, interpreted similar to a Z score[34]) greater than 3, corresponding approximately to $p < 0.001$. The bootstrap procedure also yields 99% CIs around the correlations between membership in each severity group and the pattern of regional brain volume changes. Because image-wide statistical assessment is performed in a single analytic step, no correction for multiple comparisons across brain regions is required.

Two PLS analyses were conducted. The first incorporated the full sample of 69 TBI patients, providing a global picture of severity effects on brain volumes in this sample. The second was restricted to 46 patients without traceable focal lesions, hereafter referred to as the diffuse injury group (acknowledging that the focal lesion patients also had diffuse injury). Each analysis included CSF, gray matter, and white matter volumes. Ancillary analyses were conducted on separate vCSF and sCSF volumes.

RESULTS Each PLS analysis (full sample and diffuse injury group) yielded a single latent variable delineating the relationship between injury severity and brain volumes. None of the 1,500 permutated orderings of observations produced latent variables exceeded the values of those observed. The latent variables accounted for 86% of the covariance between severity and volumetric data for the full sample and 83% for the diffuse injury group.

Contribution of TBI severity to patterns of brain volume changes. There was a stepwise, dose–response relationship between TBI severity and volume loss for both the full sample and the diffuse injury group. The contribution of each TBI severity group to the patterns of volumetric changes described in the following section can be determined by examining the correlations and their 99% CI error bars as plotted in the upper left panel of figure 3, which displays results for the diffuse injury group (the pattern of group differences for the full sample was nearly identical; figure e-1 on the *Neurology*® Web site at www.neurology.org). Correlations for all TBI severity groups were reliably different from zero (i.e., the error bars did not overlap with zero), indicating that all TBI severity groups contributed significantly to the identified patterns of volume changes, with membership in the moderate to severe TBI groups associated with greater volume loss relative to the membership in the mild TBI and noninjured groups. Correlations for the moderate TBI group were nonsignificantly lower than for the severe TBI group (i.e., the error bars for these two groups overlapped). Otherwise, all group differences in correlations were significant (i.e., they had nonoverlapping error bars): the correlations for mild, moderate, and severe TBI groups were reliably different from that of the noninjured group, and correlations for the moderate and severe TBI groups were reliably different from that of the mild TBI group.

Patterns of volumetric changes. The color-coded plots of bootstrap ratios in figure 3 indicate the patterns of CSF, white matter, and gray matter volume changes associated with the above-described pattern of TBI severity group differences in the diffuse injury group (results for the full sample are presented in figure e-1). Overall, patterns of volume changes followed the known distribution of ventral frontal and temporal dam-

Figure 3 Latent variable from partial least squares analysis indicating the association of TBI severity in the diffuse injury group with patterns of volume changes across CSF, gray matter, and white matter

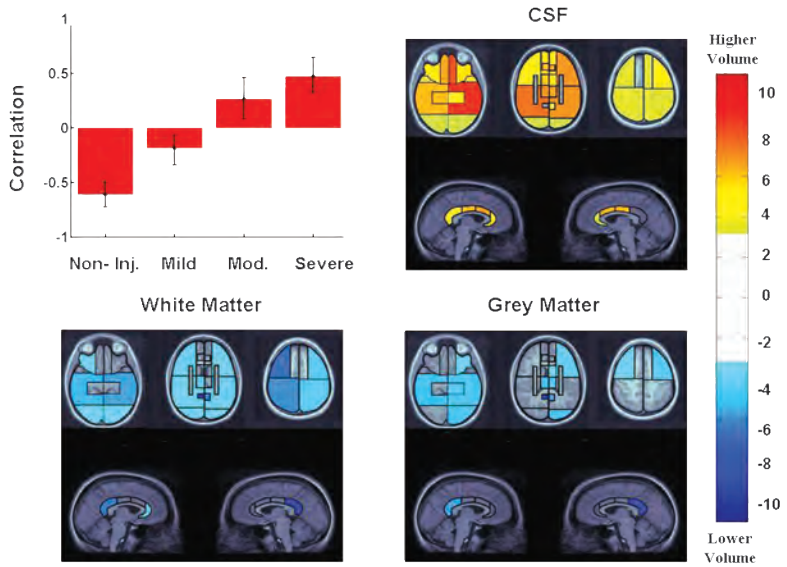

Top left: Group pattern associated with the latent variable, expressed as correlations of group membership (coded as 1 or 0) with the pattern of volume changes. Error bars represent 99% CIs. Group differences are indicated by nonoverlapping error bars. Remaining panels: Regional plots of bootstrap ratios indicating pattern of CSF (top right), white matter (bottom left), and gray matter (bottom right). The color bar indicates the coding scheme according to the level of the bootstrap ratio, interpreted similar to a *Z* score. CSF values are positive, indicating volume increases associated with traumatic brain injury (TBI) severity, whereas gray and white matter values are negative, indicating volume loss associated with TBI severity. Images were thresholded at a bootstrap ratio of 3.0, corresponding approximately to $p < 0.001$. Axial images are displayed in radiologic convention (right hemisphere displayed on left side of image). The right cingulate volume is displayed on the right side of the images, and the left cingulate volume is displayed on the left side of the images.

age in TBI,[4,5] but the changes were not restricted to these regions.

CSF increases were observed for nearly every region. These were maximal in the left medial ventral frontal and posterior temporal regions. High bootstrap values were also observed for the remaining ventral frontal, left lateral middle frontal, right medial and posterior temporal, bilateral inferior parietal, bilateral posterior basal ganglia/thalamic, and anterior and middle cingulate regions. Lower (although still significant) bootstrap values were observed in all of the remaining regions except the right superior medial frontal, right posterior cingulate, and bilateral external capsule/corona radiata regions.

White matter volume loss was also widespread, greatest in the lateral superior frontal, superior parietal, posterior temporal, and posterior cingulate regions bilaterally, with a tendency toward greater volume loss in the right hemisphere. Significant changes were also noted for the inferior frontal (right lateral), middle frontal (bilateral lateral), bilateral inferior parietal, bilateral occipital, right posterior basal ganglia/thalamic, and left anterior cingulate regions.

Gray matter volume changes were observed in a more restricted pattern, with the strongest effects observed in the posterior cingulate/retrosplenial region, right greater than left. Significant effects were also noted for ventral frontal (left lateral), middle frontal (left lateral), superior frontal (bilateral lateral), bilateral posterior temporal, left medial temporal, left occipital, and basal ganglia/thalamic regions.

As seen in figure e-1, the patterns of volumetric changes were similar for the full sample and the diffuse injury group. Bootstrap ratio maxima for the full sample generally reflected stronger effects, particularly over medial frontal and medial temporal regions. Although more robust effects are expected with the increased n of the full sample, further enhancement of parenchymal volume loss in the right ventral frontal regions corresponded to the location of FCCs (figure 1).

Ventricular vs sulcal/subdural CSF. As above, PLS analyses for the full sample and diffuse injury group yielded a single latent variable for each compartment, significant by permutation test, $p < 0.001$, with covariance between severity and volumetric data ranging between 87% and 91%. Overall, sCSF was more sensitive to group differences than was vCSF. sCSF volume in both the full sample and diffuse injury samples reliably differentiated the moderate and severe TBI groups from the mild TBI and noninjured groups, whereas vCSF only differentiated between the noninjured and severe TBI groups. The spatial distributions of sCSF and vCSF volume loss were mainly uniform, with nearly all regions in both compartments significantly contributing to the pattern.

DISCUSSION Advances in neuroimage analysis technologies have enhanced regional quantification of stable TBI neuropathology through volumetric analysis of tissue compartments. Few studies have applied such methods to a well-characterized sample of TBI patients of this size. This study demonstrates systematic relationships between TBI severity and patterns of spatially extensive regional volumetric changes in the brain. The patterns of volume loss demonstrated here correspond with the substantial handicap experienced in patients with TBI, even in the absence of FCC, particularly with respect to cognitive and emotional functioning.[2]

Our analyses indicated a stepwise, dose–response relationship between parenchymal volume

loss and TBI severity. Importantly, the systematic brain volume reduction with increasing TBI severity was not modeled a priori in the form of statistical contrasts as in standard univariate methods; it was rather determined statistically from covariance patterns in multivariate analysis. As expected, patients with severe TBI contributed most to the pattern of volume loss. Although the moderate TBI group showed a lesser degree of volume loss, this effect could not be statistically differentiated from the severe TBI group, suggesting that, from the perspective of volume loss, these two groups can be considered together.

The mild TBI group, although differentiated from the moderate and severe TBI groups, nonetheless contributed significantly to the pattern of volumetric changes such that this group was reliably differentiated from the noninjured group. All patients in this study sustained a TBI sufficient to warrant hospital admission; our findings do not apply to nonhospitalized mild TBI patients. Although it is possible that our mild TBI group contains patients with more significant TBI, those with extended post-traumatic amnesia or loss of consciousness were reclassified to the moderate group. The majority (69%) of these patients had the maximum GCS score of 15. One caveat to this finding is that the TBI patients were not matched to the noninjured group for socioeconomic status. Therefore, cohort effects cannot be ruled out as contributing to the differentiation between the mild TBI and noninjured groups. This caveat, of course, does not apply to the significant differentiation of the mild from the moderate and severe TBI groups that were closely matched to each other.

Although FCC undoubtedly contributes to morbidity after TBI, we found that the effects of TBI severity on volume loss held even when patients with FCC were excluded from the analysis. Indices of altered consciousness at the time of injury, such as the GCS, post-traumatic amnesia, and duration of loss of consciousness, are commonly used to classify patients in the chronic phase. Although these measures can be regarded as indirect indices of DAI burden,[39] they can be influenced by other factors. Brain integrity as quantified on chronic-phase MRI is a more sensitive and specific indicator of DAI effects. Quantification is paramount because the subtle TBI-related changes in regional patterns of volume loss may not be appreciated by the naked eye.[40]

Volume loss was spatially extensive, with nearly every region showing a significant relationship to TBI severity in at least one of the two main analyses. Nonetheless, there was a degree of spatial specificity. These findings highlight the importance of regional assessment across the whole brain, as opposed to targeted regional volumetrics.[15,41] FCCs contributed to robust effects in right ventral frontal regions in the full sample. The inclusion of patients both with and without FCC is common practice in studies of TBI. Although this practice is useful from a clinical perspective, it confounds two separate pathologies. As shown here, excluding patients with FCC can lead to separate, although overlapping, conclusions.

The spatial breadth of TBI-related volume loss confirms previous findings that DAI can be observed throughout the cerebrum[11] beyond the well-described corpus callosum, rostral brainstem, and cerebral white matter locations.[10] Consistent with a rostrocaudal gradient of TBI-related damage,[42] the most reliable effects were observed in the frontal lobes, cingulate regions, and temporal lobes, pointing to the effects of DAI on executive functions and memory. One exception to this gradient was the posterior cingulate/retrosplenial region, where gray and white matter volumes were strongly related to TBI severity, consistent with the sensitivity of a proximal region, the splenium of the corpus callosum, to TBI.[4] The posterior cingulate gyrus/retrosplenial cortex is closely functionally connected to the medial temporal lobes, frontal lobes, and anterior cingulate gyrus and is involved in cognitive and mnemonic integration.[43] This region figured prominently in a regional pattern of volume loss that covaried with performance on tests of memory and attention in a separate study with this sample (Levine et al., unpublished).

Many studies of TBI neuropathology have focused on white matter loss.[41] When both gray and white matter are probed using tissue compartment segmentation, however, effects are seen in both compartments.[17,19] Although white matter volume loss was observed in a greater number of regions than gray matter volume loss (particularly in superior and posterior regions), gray matter loss was nonetheless marked. Localized gray matter volume loss may have greater implications for specific behavioral changes than localized white matter volume loss (Levine et al., unpublished).[44]

A unique aspect of this study is the dissociation of vCSF from sCSF, facilitated by enhanced preservation of subdural CSF in our brain extraction process.[23,24] Contrary to previous studies emphasizing ventricular expansion,[16,45] we found that sCSF was more sensitive to TBI severity (see reference 24 for a similar finding in normal ag-

ing). vCSF has been related to white matter integrity.[45] Considering patients without focal lesions, vCSF in our sample was correlated (using nonparametric Pearson correlation) with total white matter volume, $r(46) = -0.50$, $p < 0.0005$; it was correlated to a lesser degree with total gray matter volume, $r(46) = -0.32$, $p < 0.05$. The correlation of sCSF to total white matter volume was similar to that of vCSF, $r(46) = -0.47$, $p < 0.005$, whereas the correlation between sCSF and gray matter volume was quite robust, $r(46) = -0.74$, $p < 0.0005$. Therefore, although sCSF and vCSF show expected differential relationships to gray and white matter volume, this dissociation is not complete.

Although our sample size was large compared with previous studies, the size of TBI severity groups (particularly the mild group) was small. The current study did not concern the significance of volume loss on behavior, a topic that we are currently exploring in this same sample of TBI patients. Although our image analysis pipeline is automated, flexible, and well-suited to patients with distorted brain anatomy, it lacks the anatomic precision of manual tracing and the spatial resolution of voxel-based methods. A fuller appreciation of brain-behavior effects in TBI will require additional imaging technologies, such as functional neuroimaging,[40] diffusion tensor imaging,[46] and MR spectroscopy.[47]

ACKNOWLEDGMENT

The authors thank Maroquine Aziz, Ann Campbell, Catherine Hynes, Sabitha Kanagasabai, Marina Mandic, Colleen O'Toole, Karen Philp, Adriana Restagno, Joel Ramirez, Pheth Sengdy, Philip Sharkey, Jovanka Skocic, and Gary Turner for technical assistance; Esther Fujiwara and A. Randall McIntosh for assistance with the PLS analyses; and the TBI patients and noninjured volunteers for participating in this research.

Received March 28, 2007. Accepted in final form August 30, 2007.

REFERENCES

1. Hirtz D, Thurman DJ, Gwinn-Hardy K, Mohamed M, Chaudhuri AR, Zalutsky R. How common are the "common" neurologic disorders? Neurology 2007;68:326–337.
2. National Center for Injury Prevention and Control. Traumatic Brain Injury in the United States: A Report to Congress. Atlanta: Centers for Disease Control and Prevention, 1999.
3. Dikmen SS, Ross BL, Machamer JE, Temkin NR. One year psychosocial outcome in head injury. J Int Neuropsychol Soc 1995;1:67–77.
4. Gentry LR, Godersky JC, Thompson B. MR imaging of head trauma: review of the distribution and radiopathologic features of traumatic lesions. Am J Neuroradiol 1988;9:101–110.
5. Courville CB. Pathology of the Central Nervous System. Part 4. Mountain View, CA: Pacific Press Publishing, 1937.
6. Ommaya AK, Gennarelli TA. Cerebral concussion and traumatic unconsciousness: correlation of experimental and clinical observations of blunt head injuries. Brain 1974;97:633–654.
7. Povlishock JT, Christman CW. The pathobiology of traumatically induced axonal injury in animals and humans: a review of current thoughts. J Neurotrauma 1995;12:555–564.
8. Bigler ED. Brain imaging and behavioral outcome in traumatic brain injury. J Learn Disabil 1996;29:515–530.
9. Gentry LR. Head trauma. In: Atlas SW, ed. Magnetic Resonance Imaging of the Brain and Spine. New York: Raven, 1990:439–466.
10. Adams JH, Graham DI, Murray LS, Scott G. Diffuse axonal injury due to nonmissile head injury in humans: an analysis of 45 cases. Ann Neurol 1982;12:557–563.
11. Povlishock JT. Pathobiology of traumatically induced axonal injury in animals and man. Ann Emerg Med 1993;22:980–986.
12. Levin HS, Meyers CA, Grossman RG, Sarwar M. Ventricular enlargement after closed head injury. Arch Neurol 1981;38:623–629.
13. Levin HS, Williams DH, Valastro M, Eisenberg HM, Crofford MJ, Handel SF. Corpus callosal atrophy following closed head injury: detection with magnetic resonance imaging. J Neurosurg 1990;73:77–81.
14. Gale SD, Johnson SC, Bigler ED, Blatter DD. Trauma-induced degenerative changes in brain injury: a morphometric analysis of three patients with preinjury and postinjury MR scans. J Neurotrauma 1995;12:151–158.
15. Tomaiuolo F, Carlesimo GA, Di Paola M, et al. Gross morphology and morphometric sequelae in the hippocampus, fornix, and corpus callosum of patients with severe non-missile traumatic brain injury without macroscopically detectable lesions: a T1 weighted MRI study. J Neurol Neurosurg Psychiatry 2004;75:1314–1322.
16. Blatter DD, Bigler ED, Gale SD, et al. MR-based brain and cerebrospinal fluid measurement after traumatic brain injury: correlation with neuropsychological outcome. AJNR Am J Neuroradiol 1997;18:1–10.
17. Serra-Grabulosa JM, Junque C, Verger K, Salgado-Pineda P, Maneru C, Mercader JM. Cerebral correlates of declarative memory dysfunctions in early traumatic brain injury. J Neurol Neurosurg Psychiatry 2005;76:129–131.
18. Berryhill P, Lilly MA, Levin HS, et al. Frontal lobe changes after severe diffuse closed head injury in children: a volumetric study of magnetic resonance imaging. Neurosurgery 1995;37:392–399.
19. Wilde EA, Hunter JV, Newsome MR, et al. Frontal and temporal morphometric findings on MRI in children after moderate to severe traumatic brain injury. J Neurotrauma 2005;22:333–344.
20. Gale SD, Baxter L, Roundy N, Johnson SC. Traumatic brain injury and grey matter concentration: a preliminary voxel based morphometry study. J Neurol Neurosurg Psychiatry 2005;76:984–988.
21. Tomaiuolo F, Worsley KJ, Lerch J, et al. Changes in white matter in long-term survivors of severe non-

missile traumatic brain injury: a computational analysis of magnetic resonance images. J Neurotrauma 2005; 22:76–82.
22. Teasdale G, Jennett B. Assessment of coma and impaired consciousness: a practical scale. Lancet 1974;2: 81–84.
23. Kovacevic N, Lobaugh NJ, Bronskill MJ, Levine B, Feinstein A, Black SE. A robust method for extraction and automatic segmentation of brain images. Neuroimage 2002;17:1087–1100.
24. Dade LA, Gao FQ, Kovacevic N, et al. Semiautomatic brain region extraction: a method of parcellating brain regions from structural magnetic resonance images. Neuroimage 2004;22:1492–1502.
25. Kovacevic N, Henderson JT, Chan E, et al. A three-dimensional MRI atlas of the mouse brain with estimates of the average and variability. Cereb Cortex 2005;15:639–645.
26. Woods RP, Grafton ST, Holmes CJ, Cherry SR, Mazziotta JC. Automated image registration: I. General methods and intrasubject, intramodality validation. J Comput Assist Tomogr 1998;22:139–152.
27. Woods RP, Grafton ST, Watson JD, Sicotte NL, Mazziotta JC. Automated image registration: II. Intersubject validation of linear and nonlinear models. J Comput Assist Tomogr 1998;22:153–165.
28. Collins DL, Evans AC. ANIMAL: validation and applications of non-linear registration based segmentation. Int J Pattern Recogn 1997;11:1271–1294.
29. Talairach J, Tournoux P. Co-planar Stereotaxic Atlas of the Human Brain. Stuttgart: Georg Thieme Verlag, 1988.
30. Arndt S, Cohen G, Alliger RJ, Swayze VW II, Andreasen NC. Problems with ratio and proportion measures of imaged cerebral structures. Psychiatry Res Neuroimaging 1991;40:79–89.
31. Feinstein A, Roy P, Lobaugh N, Feinstein K, O'Connor P, Black S. Structural brain abnormalities in multiple sclerosis patients with major depression. Neurology 2004;62:586–590.
32. Gilboa A, Ramirez J, Kohler S, Westmacott R, Black SE, Moscovitch M. Retrieval of autobiographical memory in Alzheimer's disease: relation to volumes of medial temporal lobe and other structures. Hippocampus 2005;15:535–550.
33. McIntosh AR, Bookstein FL, Haxby JV, Grady CL. Spatial pattern analysis of functional brain images using partial least squares. Neuroimage 1996;3:143–157.
34. McIntosh AR, Lobaugh NJ. Partial least squares analysis of neuroimaging data: applications and advances. Neuroimage 2004;23 (suppl 1):S250–S263.
35. Itier RJ, Taylor MJ, Lobaugh NJ. Spatiotemporal analysis of event-related potentials to upright, inverted, and contrast-reversed faces: effects on encoding and recognition. Psychophysiology 2004;41:643–653.
36. Lobaugh NJ, West R, McIntosh AR. Spatiotemporal analysis of experimental differences in event-related potential data with partial least squares. Psychophysiology 2001;38:517–530.
37. Edgington ES. Randomization Tests. New York: Marcel Dekker, 1980.
38. Wasserman S, Bockenholt U. Bootstrapping: applications to psychophysiology. Psychophysiology 1989;26: 208–221.
39. Gennarelli TA, Thibault LE, Adams JH, Graham DI, Thompson CJ, Marcincin RP. Diffuse axonal injury and traumatic coma in the primate. Ann Neurol 1982; 1982:564–572.
40. Levine B, Fujiwara E, O'Connor C, et al. In vivo characterization of traumatic brain injury neuropathology with structural and functional neuroimaging. J Neurotrauma 2006;23:1396–1411.
41. Gale SD, Johnson SC, Bigler ED, Blatter DD. Nonspecific white matter degeneration following traumatic brain injury. J Int Neuropsychol Soc 1995;1:17–28.
42. Wilson J. The relationship between neuropsychological function and brain damage detected by neuroimaging after closed head injury. Brain Injury 1990;4:349–363.
43. Morris R, Pandya DN, Petrides M. Fiber system linking the mid-dorsolateral frontal cortex with the retrosplenial/presubicular region in the rhesus monkey. J Comp Neurol 1999;407:183–192.
44. Fujiwara E, Schwartz ML, Gao F, Black SE, Levine B. Ventral frontal cortex functions and quantified MRI in traumatic brain injury. Neuropsychologia (in press).
45. Anderson CV, Bigler ED. The role of caudate nucleus and corpus callosum atrophy in trauma-induced anterior horn dilation. Brain Injury 1994;8:565–569.
46. Arfanakis K, Haughton VM, Carew JD, Rogers BP, Dempsey RJ, Meyerand ME. Diffusion tensor MR imaging in diffuse axonal injury. AJNR Am J Neuroradiol 2002;23:794–802.
47. Garnett MR, Blamire AM, Rajagopalan B, Styles P, Cadoux-Hudson TA. Evidence for cellular damage in normal-appearing white matter correlates with injury severity in patients following traumatic brain injury: a magnetic resonance spectroscopy study. Brain 2000; 123 (pt 7):1403–1409.